atmosphere

MDPI

Article

Suitability of CMIP6 Models Considering Statistical Downscaling Based on GloH2O and E-OBS Dataset in River Basin Districts of the Southeastern Baltic Sea Basin

Vytautas Akstinas *, Karolina Gurjazkaitė, Diana Meilutytė-Lukauskienė and Darius Jakimavičius

Laboratory of Hydrology, Lithuanian Energy Institute, Breslaujos St. 3, LT-44403 Kaunas, Lithuania; karolina.gurjazkaite@lei.lt (K.G.); diana.meilutyte-lukauskiene@lei.lt (D.M.-L.); darius.jakimavicius@lei.lt (D.J.)
* Correspondence: vytautas.akstinas@lei.lt

Abstract: Climate projections based on global climate models (GCMs) are generally subject to large uncertainties, as the models only reflect the local climate in the past to a limited extent. Statistical downscaling is the most cost-effective approach to identify the systematic biases of the GCMs from the past and eliminate them in the projections. This study seeks to evaluate the effectiveness of GCMs in capturing local climatic characteristics at the river basin district scale by applying gridded statistical downscaling techniques using global and regional datasets. The historical observational datasets E-OBS and GloH2O were selected to downscale the raw data of 17 GCMs from ~1° grid cells to 0.25° resolution. E-OBS is a regional dataset supported by a dense network of meteorological stations in Europe, while GloH2O is a global dataset covering all continents. The results show that the suitability of the GCMs varies depending on the selected parameter. The statistical downscaling revealed the advantages of the performance of E-OBS in representing local climate characteristics during the historical period and emphasized the crucial role of regional datasets for good climate depiction. Such an approach provides the possibility to assess the relative performance of GCMs based on the high-resolution observational and reanalysis datasets, while generating statistically downscaled datasets for the best ranked GCMs. The strategies used in this study can help to identify the most appropriate models to assemble the right ensemble of GCMs for specific studies.

Keywords: statistical downscaling; CMIP6; BCCAQ; E-OBS; GloH2O; Baltic Sea basin

check for updates

Academic Editor: Nicola Scafetta

Received: 26 November 2024
Revised: 12 February 2025
Accepted: 14 February 2025
Published: 18 February 2025

Citation: Akstinas, V.; Gurjazkaitė, K.; Meilutytė-Lukauskienė, D.; Jakimavičius, D. Suitability of CMIP6 Models Considering Statistical Downscaling Based on GloH2O and E-OBS Dataset in River Basin Districts of the Southeastern Baltic Sea Basin. *Atmosphere* **2025**, *16*, 229. https://doi.org/10.3390/atmos16020229

Copyright: © 2025 by the authors. Licensee MDPI, Basel, Switzerland. This article is an open access article distributed under the terms and conditions of the Creative Commons Attribution (CC BY) license (https://creativecommons.org/licenses/by/4.0/).

1. Introduction

Reliable information on historical and future regional and local climate change is essential for effective climate change risk management. Global climate models (GCMs) can reproduce past climate characteristics and project future climate development. They are currently one of the most effective tools for climate change research [1]. However, we should not overlook the fact that these projections usually have a relatively coarse spatial resolution and are subject to significant biases and uncertainties [2]. Therefore, the direct application of GCMs at local or regional scales is usually problematic and not recommended for direct use [3,4]. To overcome these limitations, downscaling techniques are used to refine the resolution of GCM results and make them more accurate for local and regional climate studies and policy decisions [5,6]. These techniques improve the usability of GCM data by increasing spatial resolution and thereby providing more detailed and accurate climate projections for specific areas. As GCMs are developed by different organizations, their performance varies in different regions of the world [7]. These differences require a careful

and critical selection of models from the available suite for accurate climate projections. Downscaling GCM data is essential to obtain high-resolution climate information that can be used for detailed impact assessments and informed decision-making in sectors such as agriculture, water resources and energy. This process mitigates the limitations imposed by the coarse resolution and biases of GCMs and enables a more accurate understanding of climate change impacts at local and regional scales. Overall, refining the GCM results through downscaling is a crucial step towards producing reliable climate projections, which are essential for managing climate risks and formulating effective adaptation strategies.

Regional climate models (RCMs) can generate high-resolution climate projections for a region, with the latter downscaling the coarse results of the GCMs [8]. Both approaches are effective, but only the application scales and purposes differ from each other. For example, the coarse resolution of GCMs improves the accuracy of the representation of large-scale atmospheric circulation, which significantly influences modelling strategies. RCMs have the advantage of being high resolution and being able to be used on a local scale. However, RCMs are prone to significant biases, errors and sensitivity to the boundary conditions of GCMs [9]. In addition, the availability of RCMs often lags the development of the latest climate scenarios. The series of Coupled Model Intercomparison Projects (CMIP) launched by the World Climate Research Programme is currently in its sixth phase (CMIP6). There is a lack of high-resolution climate projections for CMIP6-based simulations [10]. The CMIP6 multi-model database [11] following the Shared Socio-Economic Pathway (SSP) [12] has become a new standard for investigating future climate projections, as evidenced by its use in major reports such as those of the IPCC [13]. However, the production of these projections requires a careful selection of GCMs, RCMs and SSPs with a limited number of ensemble members that can be used. Other important decisions concern the size of the spatial domains, the spatial resolution and the length of the simulations. Many of these decisions can now be standardized by international guidelines from the Coordinated Regional Climate Downscaling Experiment (CORDEX-CMIP6), which specify parameters such as spatial domains, spatial resolutions, SSP priority order and some modelling details [14]. Adherence to these international guidelines offers advantages in terms of comparability with other regions worldwide, legitimacy of an international programme and facilitation of collaboration through a common framework. However, it should be noted that there is currently no equivalent to EURO-CORDEX for SSP climate scenarios. In addition, dynamic downscaling requires considerable computational resources, which poses further challenges for the generation of high-resolution climate projections.

The results of global climate models are often too coarse to accurately capture regional and local climate details. Downscaling techniques are used to compensate for this discrepancy between scales. Downscaling is divided into two main categories: dynamic downscaling (DD) and statistical downscaling (SD). Dynamic downscaling incorporates regional climate information using large-scale GCM boundary conditions by modelling regional climate dynamics [15]. This method uses regional climate models to simulate the climate at a finer resolution and capture complex interactions and processes specific to a region. In contrast, statistical downscaling is based on empirical relationships between large-scale atmospheric variables and local surface parameters. In this method, the local climate variables are statistically related to the large-scale variables provided by the GCMs. Several statistical downscaling techniques have been developed to establish these empirical relationships. Widely used methods include the Statistical Downscaling Model (SDSM) and the stochastic weather generator LARS-WG [16]. These techniques construct climate change scenarios for daily precipitation and temperature extremes at individual locations using GCM grid point information. In addition, statistical grid downscaling was used to improve the small-scale variability of remote sensing products. By interpolating station-

based SD results, grid-based products can be derived that provide improved resolution and accuracy [17]. This approach has been applied in several studies to refine the spatial details of climate projections and remote sensing data to provide more reliable information for local-scale impact assessments and decision making [18–20].

Grid-based statistical downscaling methods are essential for processing climate model data to control distributed hydrological models [21]. Numerous studies have compared different statistical downscaling methods for climatological and hydrological projections. The Bias Correction Constructed Analogues with Quantile Mapping Reordering (BCCAQ) is one of the most advanced methods that provides a fine spatial representation and temporal variability of the downscaled parameters [21,22]. The BCCAQ method is used to downscale and correct the biases in the daily simulations of temperature and precipitation from a resolution of 10 km to 800 m, effectively reducing the observational error [23,24]. BCCAQ shows potential improvements over other station-based statistical downscaling methods, especially in the resolution of spatial gradients at the event scale [22,25]. BCCAQ has passed numerous tests for hydrological extremes and has proven its effectiveness in removing biases from GCMs and reproducing extreme events when calibrated with high-resolution reference datasets [26]. BCCAQ has been instrumental in developing high-resolution climate datasets for assessing climate extremes [23] and conducting climate change impact assessment studies [27]. Therefore, BCCAQ shows superior performance when the downscaled variables are used to simulate hydrological extremes [21].

Already available databases are based on various real observations and reanalysis datasets. For example, global downscaled data can be accessed via the Centre for Environmental Data Analysis (CEDA), which provides historical and future data with a spatial resolution of 0.25° and in daily time steps for three common Socioeconomic Pathways (SSPs) used for the EVOFLOOD project [28]. The downscaled data was based on the global GloH2O dataset. While some datasets such as GloH2O provide global coverage, the use of regional-scale databases can improve data accuracy and subsequent climate projections. A well-known historical database for climate variables in Europe is the European Observations (E-OBS), which anyone can download from the European Climate Assessment & Dataset (ECA&D) website [29]. E-OBS provides gridded climate data sets, including daily average, maximum and minimum temperatures and precipitation records. E-OBS is widely recognized for its reliability and accurately represents regional climate patterns across the European continent [30]. It serves as a cornerstone for statistical downscaling on a continental scale [31,32]. Therefore, the aim of this study is to compare the suitability of CMIP6 GCMs for representing climatic features at the river basin scale by applying gridded statistical downscaling based on the global and regional datasets to improve the historical raw GCM simulations at the river basin district level.

2. Study Area and Data

Three transboundary river basin districts, namely Nemunas, Venta and Lielupė, located in the southeastern part of the Baltic Sea basin, were selected for this study (Figure 1). Together they cover more than 138 thousand km^2. The largest of them is the Nemunas RBD, which ranks 15th in Europe and 4th in the Baltic Sea basin in terms of catchment area. The total catchment area of the Nemunas RBD is 97.9 thousand km^2. Most of it is in Lithuania and Belarus (47.6% and 46.3% respectively) and only 6.1% in Poland, Latvia and Russia. The Venta and Lielupė RBDs are significantly smaller, with an area of 22.3 thousand km^2 and 17.9 thousand km^2 respectively. These catchment areas are only shared by Lithuania and Latvia. The upper reaches and part of the middle reaches belong to Lithuanian territory, while the remaining parts are in Latvian territory. Water management in selected RBDs faces some challenges regarding guidelines for European Union (EU) countries (Lithuania,

Latvia and Poland) and separate practices in non-EU countries member, such as Belarus. Each of these countries plays an important role in the management of the water sources, as the actions and changes in one country have a cascading effect on the downstream countries. Therefore, it is important to analyze these areas as a whole and consider every possible change through consistent assessment approaches.

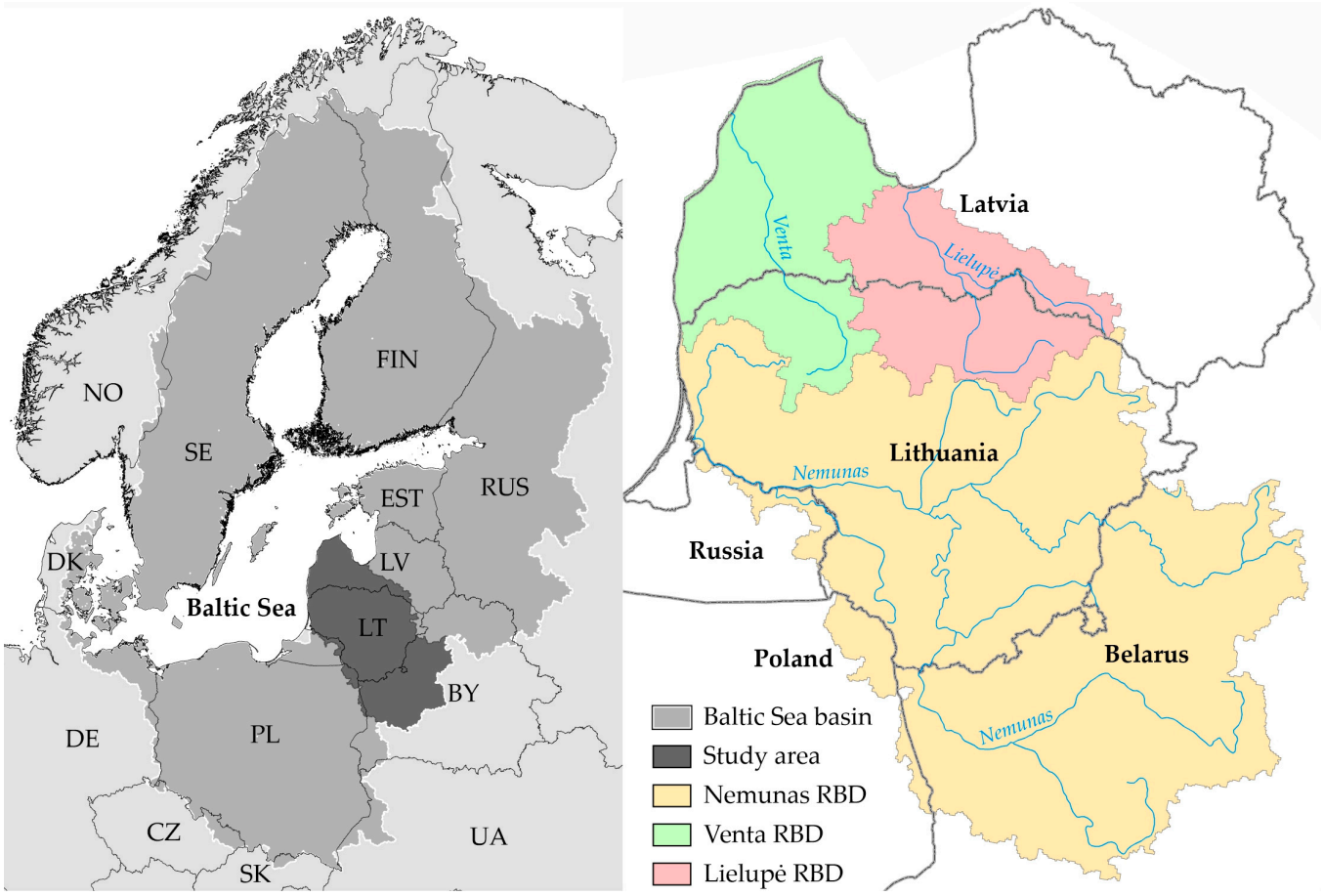

Figure 1. Study area and its location in the Baltic Sea basin.

In this study, we analyzed the average daily air temperature (T, °C) and daily precipitation (P, mm) from 17 global climate models (ACCESS-CM2, BCC-CSM2-MR, CESM2, CMCC-CM2-SR5, CMCC-ESM2, GFDL-ESM4, HadGEM3-GC31-LL, INM-CM4-8, INM-CM5-0, IPSL-CM6A-LR, KACE-1-0-G, MIROC-ES2L, MIROC6, MPI-ESM1-2-LR, MRI-ESM2-0, NorESM2-MM and UKESM1-0-LL) with raw historical (1981–2014) simulations. All selected models provide air temperature and daily precipitation projections according to the most widely used SSP scenarios (SSP1-2.6, SSP2-4.5, SSP3-7.0 and SSP5-8.5). In addition, the statistically downscaled data for the same global climate models were also used [26,28]. The data were downscaled using the BCCAQ method (Bias Correction Constructed Analogues with Quantile mapping reordering) and historical meteorological datasets with a resolution of 0.25° from the GloH2O database (http://www.gloh2o.org/mswx/, last accessed on 26 August 2024). The raw and downscaled model data were downloaded from the Centre for Environmental Data Analysis (CEDA) database (https://auth.ceda.ac.uk/, last accessed on 26 August 2024). To compare the influence of the different meteorological databases on the climate model corrections after statistical downscaling, the regional E-OBS database version 29.0 was used for the downscaling air temperature and precipitation on the same 0.25° grid cell (https://www.ecad.eu/download/ensembles/download.php, last

accessed on 26 August 2024). The results were compared in the area of the selected RBDs to determine the influence of the different databases on the GCM corrections.

3. Methods

In this study, we aim to evaluate which climate dataset, GloH2O or E-OBS, is more suitable for modeling studies when it comes to a more accurate representation of past climatic conditions in the Nemunas, Venta and Lielupė river basins districts. GloH2O Multi-Source Weather (MSWX), which supports high-resolution (0.1°) meteorological data from 1979 to 7 months after present. Statistically downscaled data based on the GloH2O dataset were introduced by [26,28], which we specifically used in this study. E-OBS are gridded data supporting historical daily meteorological observations from a dense network of meteorological stations across Europe. Based on the E-OBS database, the raw outputs data (air temperature and precipitation amount) of all 17 GCMs in this study were statistically downscaled by applying the BCCAQ (Bias Correction Constructed Analogues with Quantile mapping reordering) method [21,22]. BCCAQ is a statistical downscaling method whose application is described in detail by Gebrechorkos et al. [26]. It is a powerful hybrid statistical downscaling method that combines several downscaling techniques [23] to produce higher resolution climate data. This method addresses a common problem in the use of GCMs, namely the fact that the modelling data is generated as a low resolution data grid (typically ~1–3°). Such resolution may be sufficient for global scale studies. Nevertheless, these results are subject to significant biases and may not be reliable enough in the context of regional or local climate studies.

The basis of BCCAQ is the Bias Correction Constructed Analogues (BCCA) [33] and Bias Correction Climate Imprint (BCCI) [34], which are performed separately to increase the resolution of the daily climate variables [21]; and Quantile delta mapping (QDM) [22] enables the correction of the data. BCCAQ combines the output results of these independently run algorithms. Gebrechorkos et al. [26] describe that BCCAQ has several advantages over other methods, especially when used for the development of regional high-resolution climate datasets that reflect climatic extremes with high accuracy and allow forecasting of subsequent phenomena, such as hydrological extremes. In our study, BCCAQ allows the resolution of the GCM models to 0.25° gridded data and to remove systemic GCM biases to obtain a better representation of local climatic changes in the analyzed region.

The BCCAQ code for the R software was obtained from the Pacific Climate Impacts Consortium website (available at: https://pacificclimate.org/resources/software-library, last accessed on 26 August 2024). The documentation of the R package can be found at: https://rdrr.io/cran/ClimDown/ (last accessed on 26 August 2024). The code was applied to 17 GCMs (NetCDF files, data from 1 January 1981 to 31 December 2014) in R (version 4.3.2 from 31 October 2023) using the ClimDown package (according to the instructions at https://github.com/pacificclimate/ClimDown, last accessed on 26 August 2024).

4. Results

4.1. Air Temperature Corrections

Figure 2 shows the applied adjustments of average air temperatures for different climate models during the downscaling process using two observational datasets: E-OBS and GloH2O. The differences indicate by how many degrees the average temperature was increased or decreased compared to the raw GCM output data. Models such as HadGEM3-GC31-LL, INM-CM5-0 and MPI-ESM1-2LR showed predominantly small changes after statistical downscaling. These models required only minimal temperature corrections for both data sets, which emphasizes their robustness in capturing regional temperature patterns. In contrast, models such as CESM2, CMCC-CM2-SR5 and CMCC-ESM2 showed

an enormous reduction in simulated air temperatures by more than −3 °C. This overestimation suggests that these models are reaching their regional limits in simulating the inherent patterns of temperature, especially when compared with observational data. Similarly, models such as ACCESS-CM2 and UKESM1-0-LL are highly elevated compared to the raw output data, indicating a systematic underestimation of temperatures that requires significant upward corrections. Models such as HadGEM3-GC31-LL, KACE-1-0-G and MPI-ESM1-2LR showed only minimal corrections compared to the downscaled results of E-OBS. This suggests that E-OBS provides a more accurate observational basis for average temperature due to its dense and high-resolution network in regions such as Europe. However, models such as CESM2 and CMCC-CM2-SR5 still showed a strong decrease in air temperature despite the higher resolution of the E-OBS dataset. This indicates an overestimation of the GCMs themselves and the database used reveals their systematic biases. The GloH2O results were characterized by a stronger decrease in air temperature than in E-OBS for models that overestimated the average air temperature and by a larger increase for models that underestimated the average air temperature. In terms of spatial distribution, the northern part of the study area was characterized by an increase in air temperature, while the southern part showed a decrease after statistical downscaling. A common trend in all models is that E-OBS-induced adjustments tends to be moderate and more evenly distributed compared to GloH2O. For example, models such as BCC-CSM2-MR and HadGEM3-GC31-LL consistently showed better agreement with the E-OBS corrections. This pattern emphasizes the advantage of the dense regional coverage and finer resolution of E-OBS. In addition, models with significant biases—such as CESM2, CMCC-ESM2, CMCC-ESM2 and other overestimated models—showed their limitations regardless of the dataset used, although GloH2O exacerbated these biases.

The comparison of the downscaled models for the maximum average temperature (further maximum temperature) resulted in three groups of models, consisting of the models that were corrected least, moderately and most after statistical downscaling (Figure 3). GFDL-ESM4, HadGEM3-GC31-LL, MPI-ESM1-2LR and MRI-ESM2-0 were indicated as models for which the systematic biases were the smallest, such that the corrections to the maximum temperature during the downscaling process were only minor, mainly ±2 °C, compared to the raw output. This indicates that these models were already well calibrated before the downscaling process. On the other hand, models such as BCC-CSM2-MR, the INM family and KACE-1-0-G showed that their original simulations were significantly overestimated. Therefore, the maximum air temperatures had to be corrected downwards by more than −10 °C during the downscaling process. This pattern extended over quite large areas of the study area when using the E-OBS and GloH2O datasets. It is unlikely that these models will be able to accurately project meteorological extremes on a local scale without significant corrections. Even high improvements through statistical downscaling call into question the choice of these models in the region when high temperatures are very important for a particular study. Furthermore, the models that simulated the maximum temperatures were somewhere between the best-fit models and the models with the largest differences. The downscaled data were on average 4 or 6 °C lower than the raw simulations. When comparing the two observational datasets, E-OBS and GloH2O, for the maximum temperature corrections, we found very little difference between them for most GCMs. Both datasets showed similar regional variability in the corrected maximum air temperatures. Both databases showed that the GCMs underestimated the temperature near the Baltic Sea coast, where the temperature was corrected to be positive in most cases. This was a good example of how a relatively low resolution of the GCMs can influence local climatic features, especially the extreme parameters. However, BCC-CSM2-MR and CMCC-ESM2 showed the largest differences between the selected databases. For BCC-CSM2-MR, downscaling

based on the GloH2O database has strongly corrected the southeastern part of the study area by reducing the raw simulation of the maximum air temperature. Meanwhile, the output of CMCC-ESM2 was significantly corrected by reducing the temperature in the central and southwestern part of the region using the E-OBS database. The differences in the corrections between the databases used reached 4 °C.

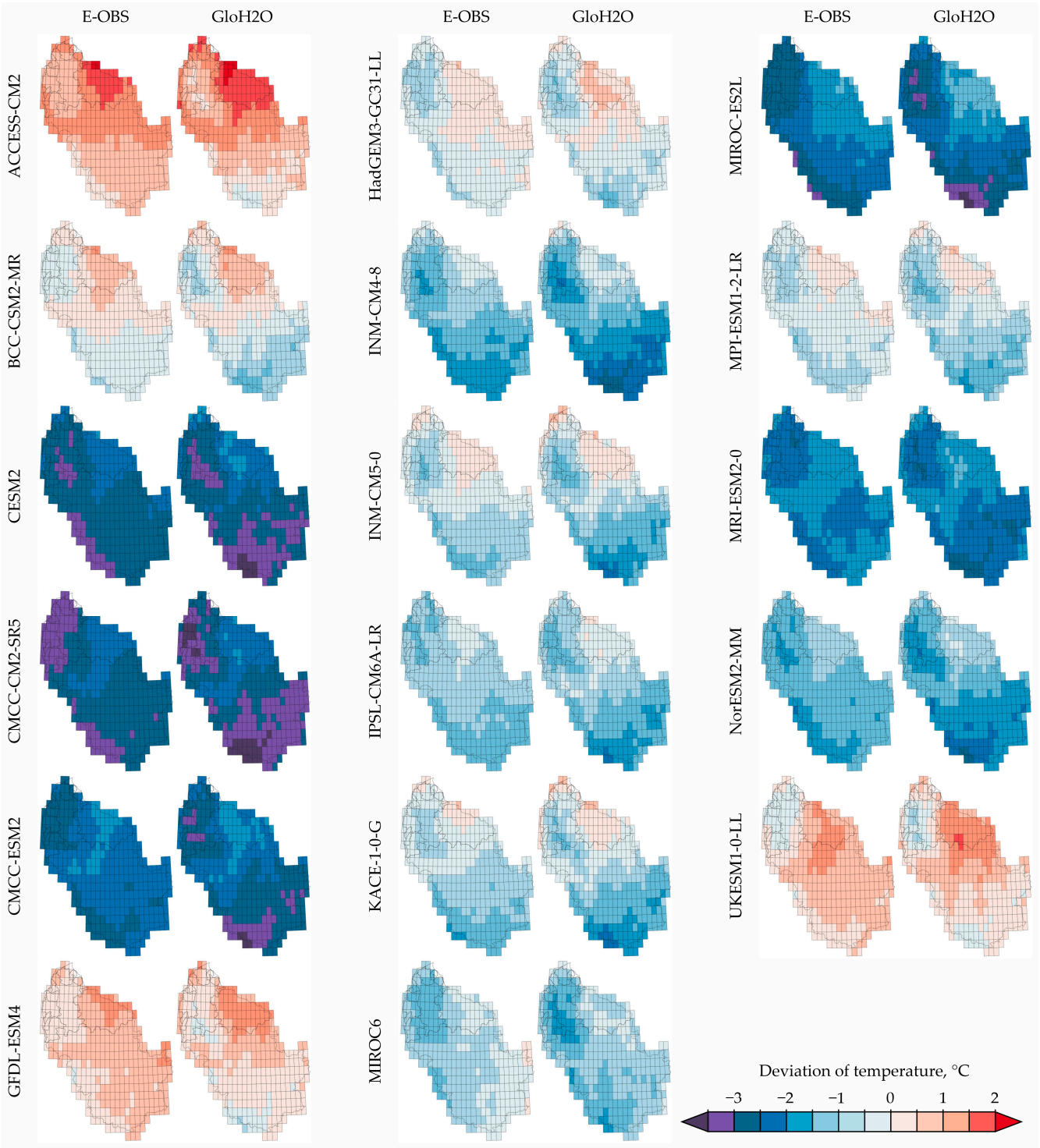

Figure 2. Change in average air temperature (°C) after the gridded statistical downscaling with the E-OBS and GloH2O datasets compared to the raw GCM output data for 1981–2014.

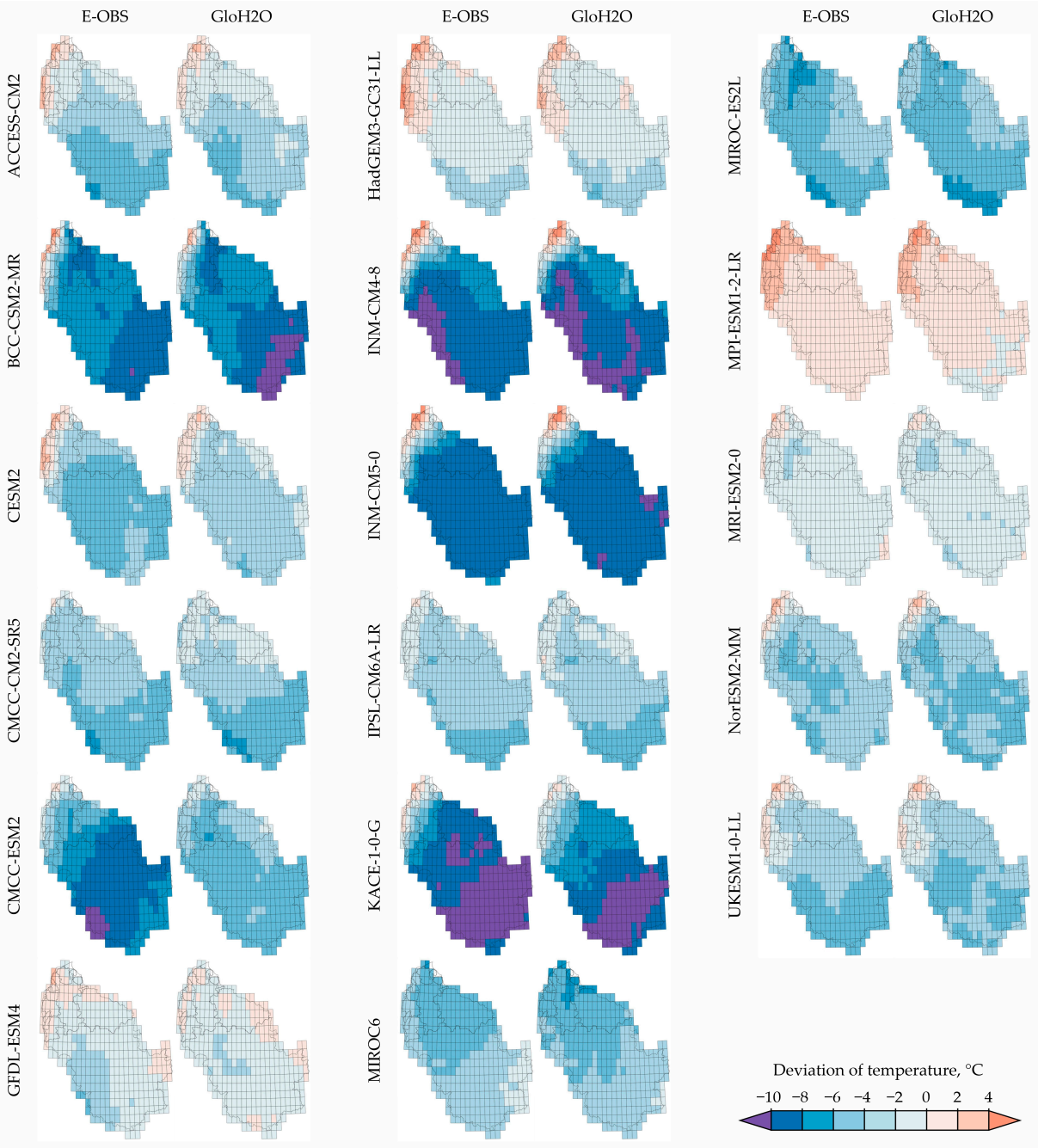

Figure 3. Change in maximum average air temperature (°C) after the gridded statistical downscaling using the E-OBS and GloH2O datasets compared to the raw GCM outputs for 1981–2014.

After statistical downscaling, models such as GFDL-ESM4 and MPI-ESM1-2LR showed predominantly small corrections in the range of ±4 °C compared to the raw simulations for the minimum average air temperature (further minimum temperature) in Figure 4. This indicates the reliability of the models in simulating the selected regional minimum temperatures. Other models such as ACCESS-CM2, HadGEM3-GC31-LL, INM-CM4-8 and MRI-ESM2-0 required additional corrections with higher improvements for an accurate representation of local climatic conditions. Regarding minimum temperatures, many climate models overestimated the western part of the area. This was clearly seen in CESM2, HadGEM3-GC31-LL, MIROC6 and MPI-ESM1-2LR. Accordingly, the minimum temperatures of the western part in CESM2 were significantly reduced by more than −14 °C to match the character of the E-OBS and GloH2O datasets. In addition, there were models

that greatly underestimated the minimum temperatures. BCC-CSM2-MR, IPSL-CM6A-LR and UKESM1-0-LL simulated minimum temperatures that were too low. As a result, significant upward corrections of more than 14 °C were made in the statistical downscaling based on the E-OBS dataset. In their raw simulations, aforementioned models delivered extremely low minimum temperatures for the study area. Consequently, their suitability is questionable even after downscaling, as the corrected systematic biases from the past are transferred to the future in climate impact assessment studies, especially if the minimum temperature plays an important role in the target object of the study. Downscaling based on the E-OBS and GloH2O datasets showed similar tendencies between the databases for most GCMs. However, BCC-CSM2-MR and KACE-1-0-G showed the largest difference between the databases, as the correction-based E-OBSs were 4 to 8 °C higher than the GloH2O-based ones for both models. The abovementioned pattern was found for the southern and southeastern part of the analyzed region. These quick corrections emphasize the importance of selecting the right data set and model combination to avoid large biases in the first steps. The fine resolution and dense observational grid of E-OBS probably help it to fit well to the observational data and minimize the required corrections, considering the unique conditions of each grid cell compared to the global dataset.

The number of days with negative air temperature was analyzed to understand the changes in air temperature distribution throughout the year after statistical downscaling, as the study area falls in the zone with warm summers and cold winters. The adjustments in air temperature varied between more than 40 days of decrease and up to 60 days of increase in days with negative temperature (Figure 5). Of all 17 selected climate models, three models such as CESM2, CMCC-CM2-SR5 and CMCC-ESM2 consistently showed large corrections on the upscaling side, indicating a significant underestimation of the number of days with negative temperatures. Accordingly, downscaling greatly increased the number of days in both the E-OBS and GloH2O datasets. The corrections fluctuated on average between 30 and 50 days, and even more than 50 days for the GloH2O database. In contrast, models such as GFDL-ESM4 and MIROC6 showed clearly negative corrections, indicating a consistent overestimation of days with negative temperatures, which had to be corrected downwards during the downscaling process to preserve the character of the data in the databases used. Despite the vast improvements mentioned above, there were 8 models (ACCESS-CM2, BCC-CSM2-MR, HadGEM3-GC31-LL, IPSL-CM6A-LR, KACE-1-0-G, MIROC-ES2L, MPI-ESM1-2LR and UKESM1-0-LL) that required only minimal corrections $\pm$10 days on average and 20 days for occasional (individual) models and their grid cells. These results emphasize the superior representation of the raw simulations of the listed models, which accurately reproduced the number of days with negative air temperature compared to the observational data. This dataset effectively captures the spatial and temporal patterns of days with negative temperatures and requires fewer adjustments during the downscaling process. In general, the adjustments made with the E-OBS datasets showed a more even distribution of corrections across the study area. Meanwhile, the GloH2O-based results showed individual grid cells or their groups with a larger increase or decrease in the number of days compared to E-OBS.

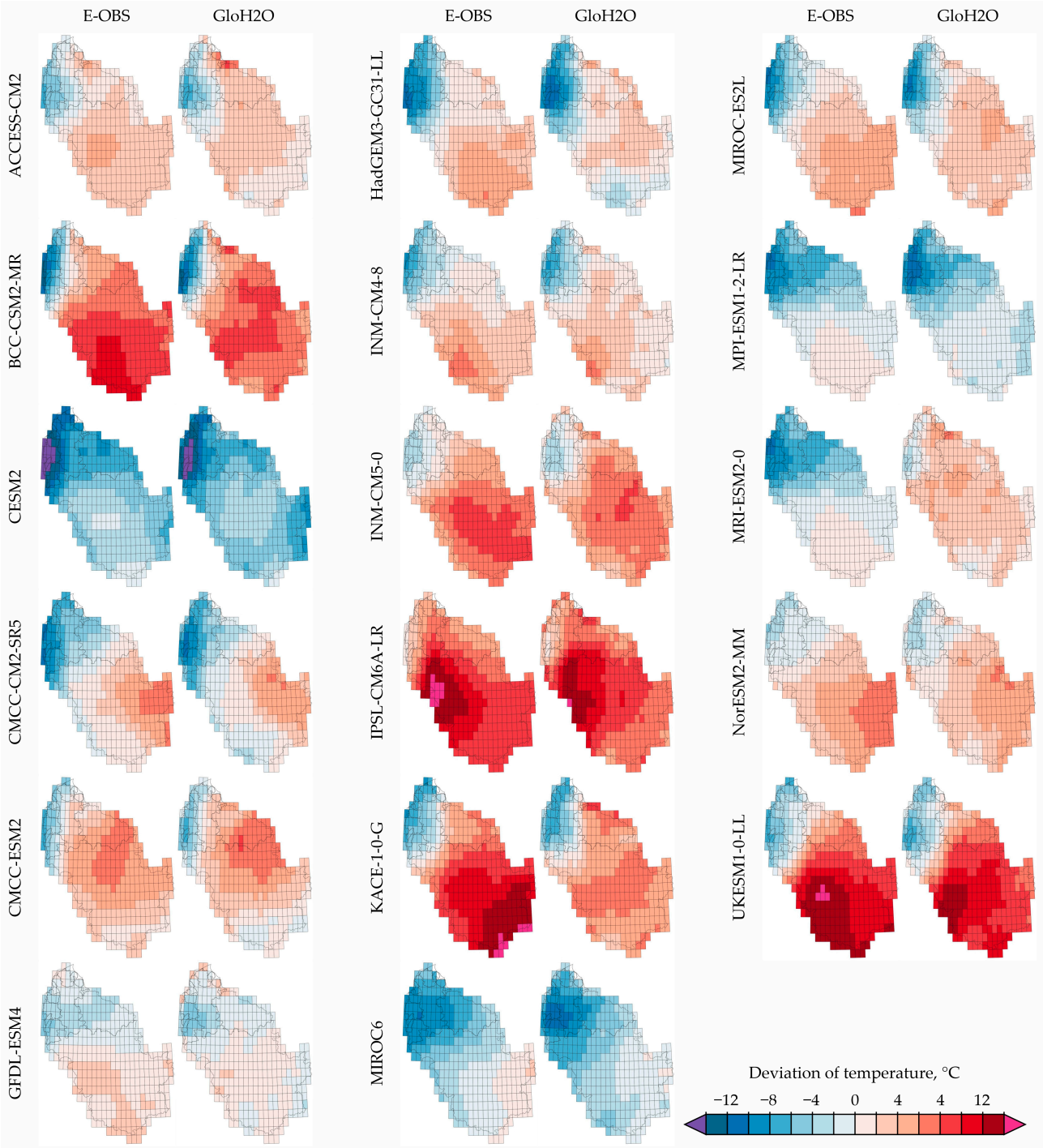

Figure 4. Change in minimum average air temperature (°C) after the gridded statistical downscaling using the E-OBS and GloH2O datasets compared to the raw GCM output for 1981–2014.

4.2. Precipitation Corrections

The trends in the downscaled precipitation data showed that several models simulated the sum of annual precipitation close to the data used in the historical reanalyzing (Figure 6). CESM2, INM-CM4-8 and NorESM2-MM showed the best performance in the largest part of the study area, which was covered by ±10% of the deviations of the downscaled data compared to the raw model results. The highest deviations were obtained in the western part of the analyzed river basins. Several groups of models were found to overestimate and underestimate annual precipitation. The group of overestimated precipitation consisted of the largest number of GCMs. GFDL-ESM4, MPI-ESM1-2-LR and MRI-ESM2-0 fell into

this group, and in some cases the statistical downscaling reduced the precipitation amount by more than 30%. This pattern was prevalent in the central and southern parts of the study area. Meanwhile, MIROC6 showed the largest amplitude between the differences in positive and negative deviations. KACE-1-0-G was the model with the highest positive precipitation corrections after statistical downscaling. Despite the background of the E-OBS or GloH2O database, the entire study area was affected by an increased precipitation amount for the KACE-1-0-G model. There was an underestimation of this parameter, especially in the western part. Most of the analyzed GCMs underestimated the precipitation character in the western part of the study area, as the upward corrections were made by statistical downscaling. The differences between the E-OBS or GloH2O databases were greater in the downscaling of precipitation than in the temperature corrections. Several common patterns were found in the climate models. Precipitation was reduced more by E-OBS in the central part of the analyzed river basins, while GloH2O increased precipitation in the southern part. The differences between these databases were on average 10 percentage points, i.e., the downscaling according to the E-OBS database was higher for negative corrections and the downscaling according to the GloH2O database was higher for positive corrections of the mentioned areas. The most significant deviations in the downscaling improvements and the largest spatial extent were found for the GFDL-ESM4, MIROC6 and MRI-ESM2-0 models.

The overall picture of maximum precipitation adjustments shows a repeating pattern in the selected GCMs. Most GCMs underestimated the extreme events; accordingly, statistical downscaling strongly increased these values, even by 100% or more (Figure 7). The strongest correction was made for the KACE-1-0-G, MIROC6, MPI-ESM1-2-LR and NorESM2-MM models, especially when downscaling according to the GloH2O database. The maximum precipitation was increased by more than 100% for many grid cells compared to the raw model data. In contrast, relatively minor improvements were made to GFDL-ESM4. The maximum precipitation corrections of this model varied between −40% and 40% compared to the raw data in most of the study area, with the exception of some grid cells in the west and east. There were also models with large differences between the downscaled data and the raw data. These differences between different parts of the selected river basins highlight the limitations of GCMs in reproducing local climatic conditions and extreme events in particular. HadGEM3-GC31-LL and INM-CM4-8 showed overestimated extremes in the eastern part and underestimated extremes in the western part, as in the case of annual precipitation. The largest differences in the downscaling results were not found between the GCMs, but between the databases used, which showed clear tendencies. The maximum precipitation downscaled according to the E-OBS database showed the smallest corrections in the raw data. Models such as CMCC-CM2-SR5, CMCC-ESM2 and GFDL-ESM4, which were downscaled according to E-OBS, did not even reach ±40% of the corrections for most of the analyzed area. On the other hand, the GloH2O-based corrections showed a drastic change for the BCC-CSM2-MR, MIROC6, MPI-ESM1-2-LR and NorESM2-MM models. The maximum precipitation of these models was increased by GloH2O. The changes were made not only for the western part of the basins, but also for the southeastern part. The differences between the two databases in terms of their application for downscaling purposes were clearly visible in the maximum precipitation. One of the databases, GloH2O, increased the extreme values to a much greater extent compared to the raw data. Downscaling based on E-OBS, on the other hand, improved the raw data to a reasonable extent, showing that this database is more suitable for the selected region to obtain the extreme values based on observations.

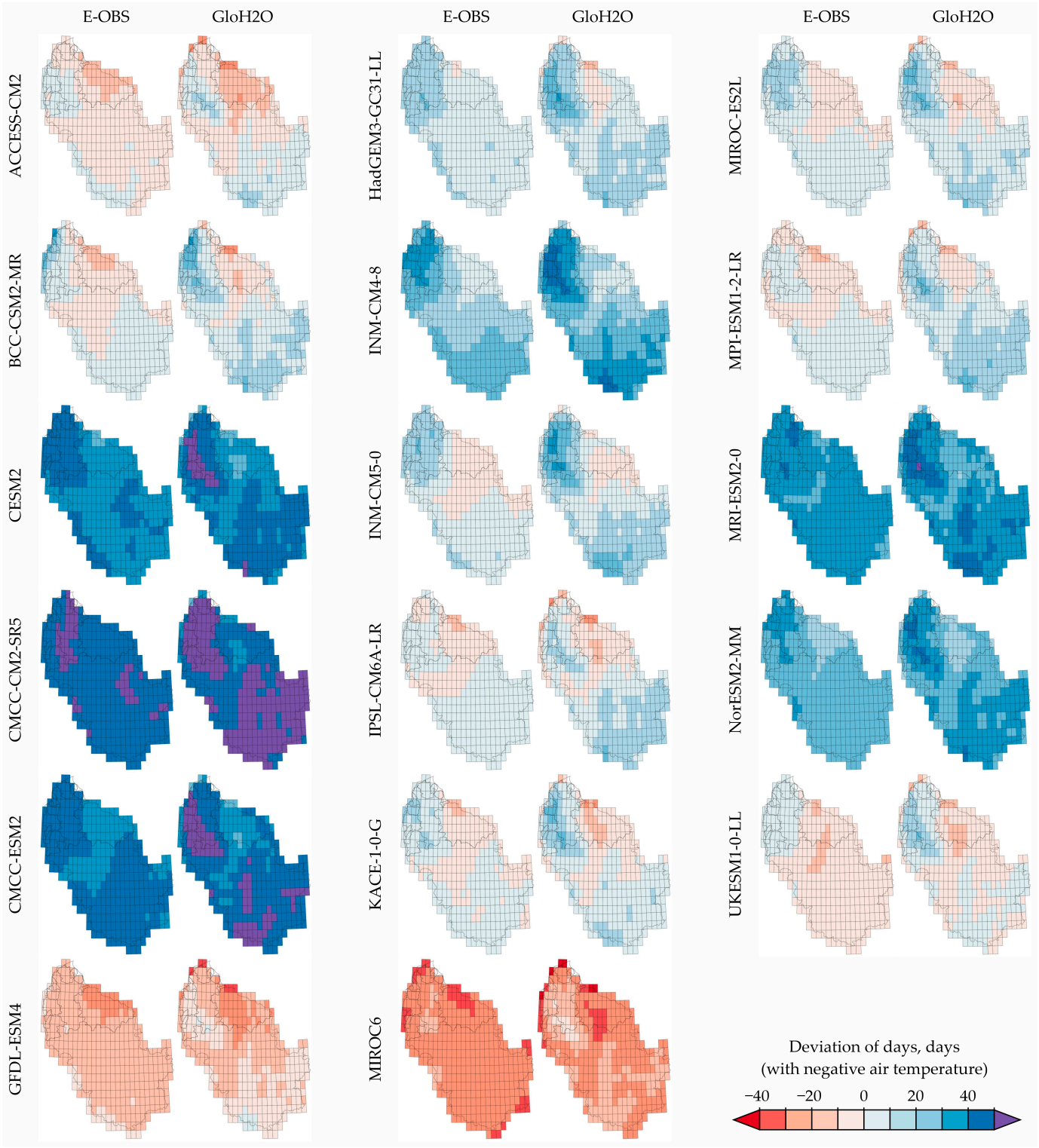

Figure 5. Change in the number of days with negative air temperature after the gridded statistical downscaling using the E-OBS and GloH2O datasets compared to the raw GCM outputs for 1981–2014.

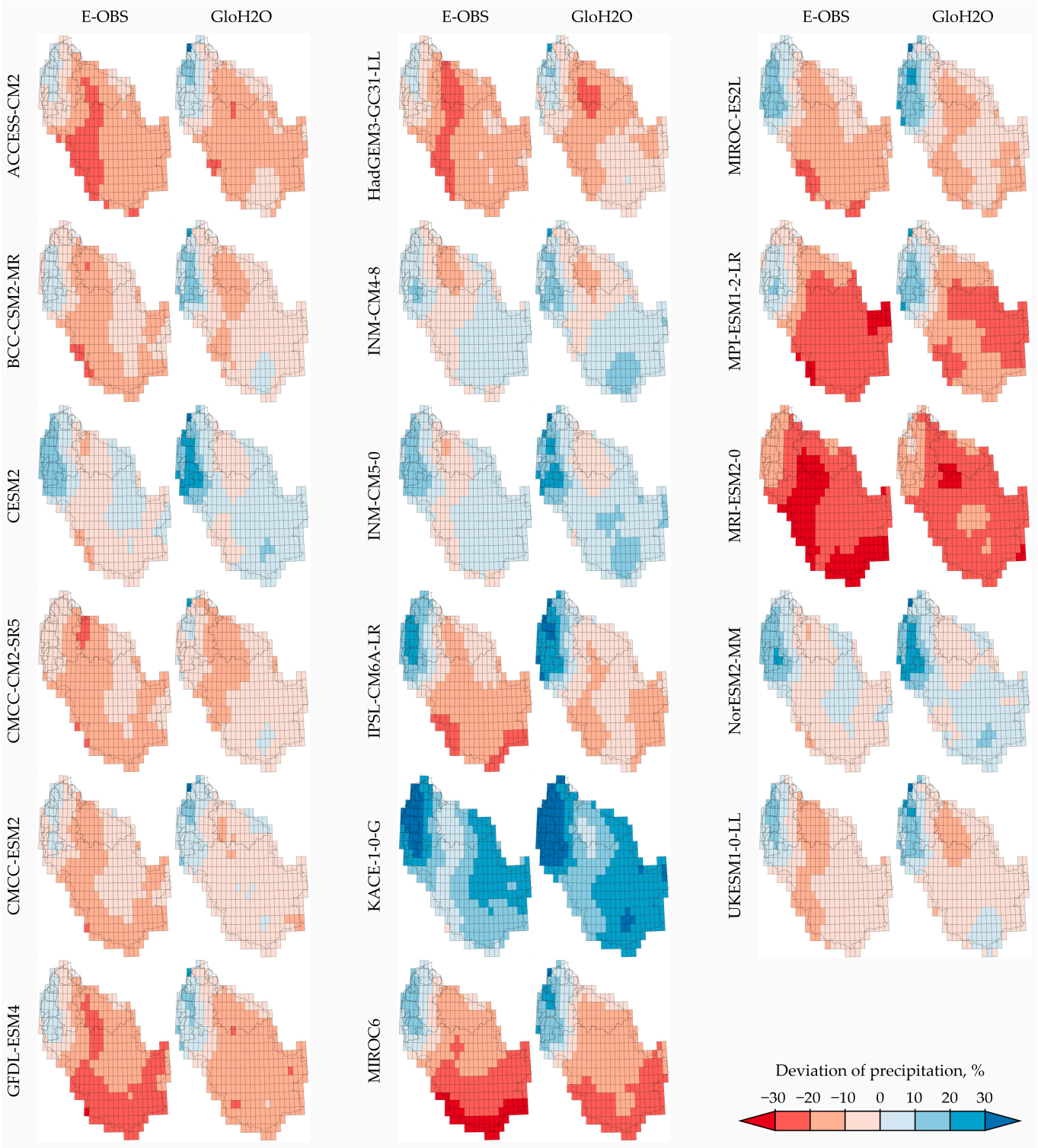

Figure 6. Change in annual precipitation (%) after the gridded statistical downscaling using the E-OBS and GloH2O datasets compared to the raw GCM output for 1981–2014.

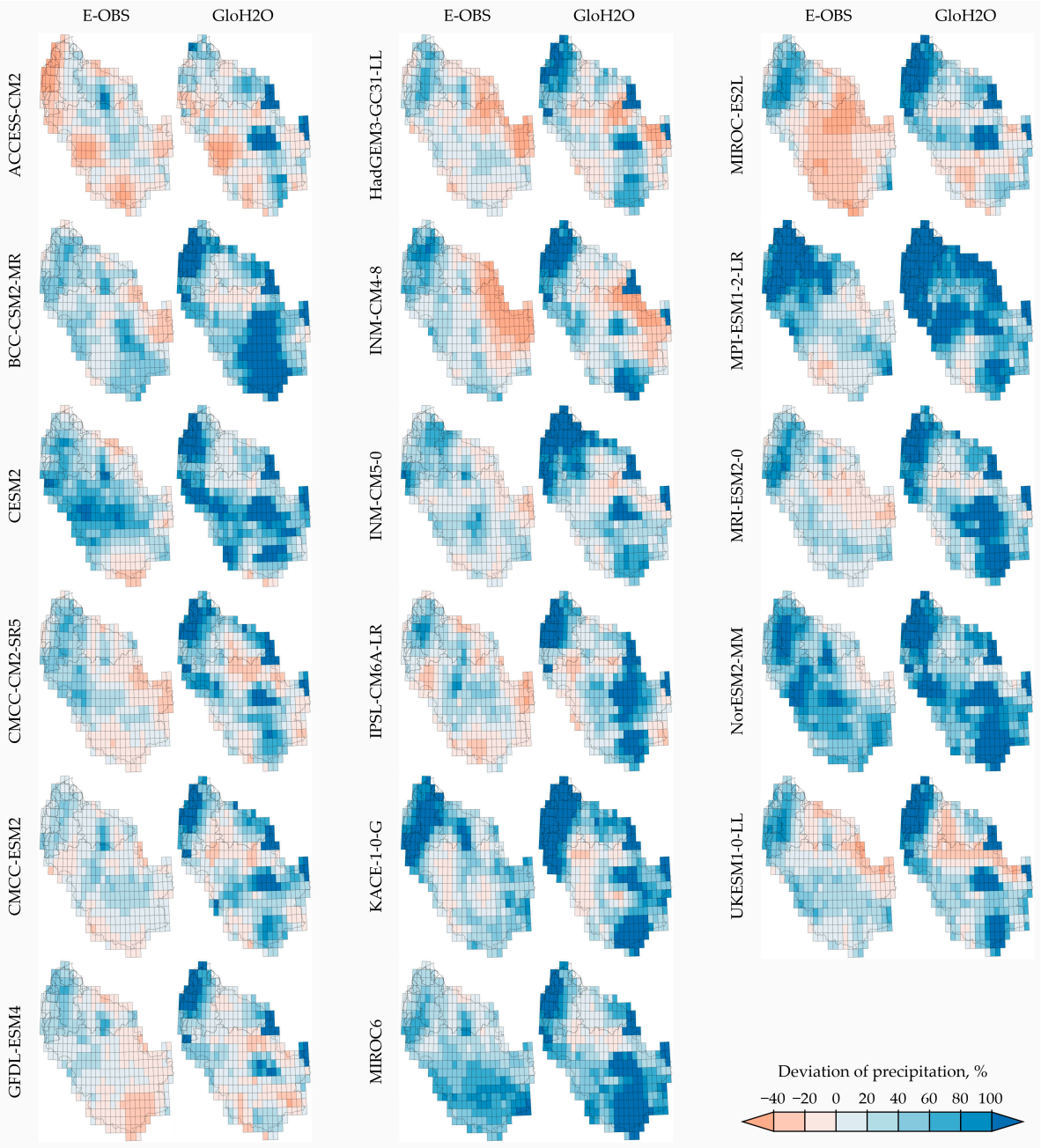

Figure 7. Change in maximum precipitation (%) after the gridded statistical downscaling using the E-OBS and GloH2O datasets compared to the raw GCM output for 1981–2014.

Considering possible hydrological studies, it is extremely important to assess the distribution of annual precipitation over the year. The same annual precipitation does not mean the same distribution patterns. Therefore, the number of dry days when precipitation is zero provides information about its allocation and intensity, because a certain amount of precipitation distributed evenly over several days has a different effect on hydrological processes than the same amount of precipitation concentrated on one day. On this basis, we tested how statistical downscaling corrects the regularities of the selected GCMs according to the E-OBS and GloH2O datasets (Figure 8). In contrast to the analysis of the previous parameters, the number of dry days (days with zero precipitation) revealed a completely different character of the corrections between the selected databases despite the differences between the models. Statistical downscaling based on E-OBS increased the number of dry days by more than 100 days per year in the raw model output. ACCESS-CM2, GFDL-

ESM4, MIROC6 and MPI-ESM1-2-LR were the models that even required an increase in the number of dry days by more than 180 days for the southern part of the study area. This indicates that the models mentioned underestimated the character of the dry days and distributed the annual precipitation evenly over the year regardless of its natural behavior. The smallest improvements were obtained for CESM2, IPSL-CM6A-LR, KACE-1-0-G and MIROC-ES2L, where the increase in the number of dry days was on average between 80 and 120 days. The GloH2O-based downscaling showed even smaller upward corrections, as the number of dry days was not increased by more than 80 days for most GCMs. For models such as IPSL-CM6A-LR, KACE-1-0-G and MIROC-ES2L, the number of dry days in individual grid cells was reduced. When comparing the two databases, the clearest systematic differences emerged and it became apparent that the E-OBS database, which is based on a dense observation network, had a much higher number of dry days than GloH2O. This could be a crucial moment in the simulation of complex hydrological processes that are sensitive to the modelling of rainfall-runoff. In this case, GloH2O had a typical character for climate models and for several models the improvements were relatively small.

4.3. Global Climate Models Biases

The spatial differences of the analyzed parameters showed the relative differences of the individual climate models within the selected region and illustrated the gradients between the different parts of the region. This only showed the ability of the model to simulate local climatic features without quantifying the suitability of the model for a specific region. Therefore, the deviations of the individual models were standardized to close this gap and to show which of the climate models required the fewest corrections during the gridded statistical downscaling (Figure 9). Depending on the selected parameter, the extent of the corrections varied between the models. There were several models that simulated the air temperature very well. GFDL-ESM4 and HadGEM3-GC31-LL were models that simulated all analyzed temperature parameters with the relatively lowest need for corrections, depending on the two historical datasets used. The CESM2 and CMCC family models, on the other hand, simulated almost all temperature parameters poorly, except for CMCC-CM2-SR5 for the minimum temperature. The models from INM-CM4-8 to KACE-1-0-G in the sequence series required large corrections for extreme values, but the average air temperature and the number of cold days were simulated relatively well. When comparing E-OBS and GloH2O, the corrections generally remained almost the same. There were large differences between E-OBS and GloH2O for the precipitation parameters, as the standardized deviations were not the same for all models. Depending on the parameter, the E-OBS-based downscaling made the smallest corrections for the maximum precipitation, while GloH2O made the smallest corrections for the number of dry days. Several climate models showed the largest differences after statistical downscaling compared to their raw simulation. Accordingly, KACE-1-0-G, MPI-ESM1-2-LR and MRI-ESM2-0 were greatly improved so that these models hardly represent the precipitation patterns over the analyzed region in their raw simulations. The aggregated values were calculated for air temperature, precipitation and their combined deviation after statistical grid downscaling to determine the suitability of the model to represent the local climatic conditions in their raw form. In addition, a ranking from the best-fit to the worst climate model was established (Figure 9). In most cases, the best models for air temperature did not show the same result for precipitation and vice versa. HadGEM3-GC31-LL, MIROC-ES2L and UKESM1-0-LL were the most balanced in terms of the parameters used. However, the overall evaluation showed that only HadGEM3-GC31-LL gained first rank position while second and third rank was given to the climate models GFDL-ESM4 and ACCESS-

CM2, which tended to be on the side of the models with higher biases in the precipitation parameters. All models in the top three places lost a little in terms of reliability in terms of precipitation and especially in the representation of the number of dry days. The MIROC-ES2L achieved fourth place. These results are very important for the formation of a possible ensemble of GCMs in climate impact assessment studies. Therefore, the prioritization of models depend on many factors and should accordingly consider the parameters essential for a particular study.



Figure 8. Change in the number of dry days (days with zero precipitation) after statistical grid downscaling using the E-OBS and GloH2O datasets compared to the raw GCM outputs for 1981–2014.

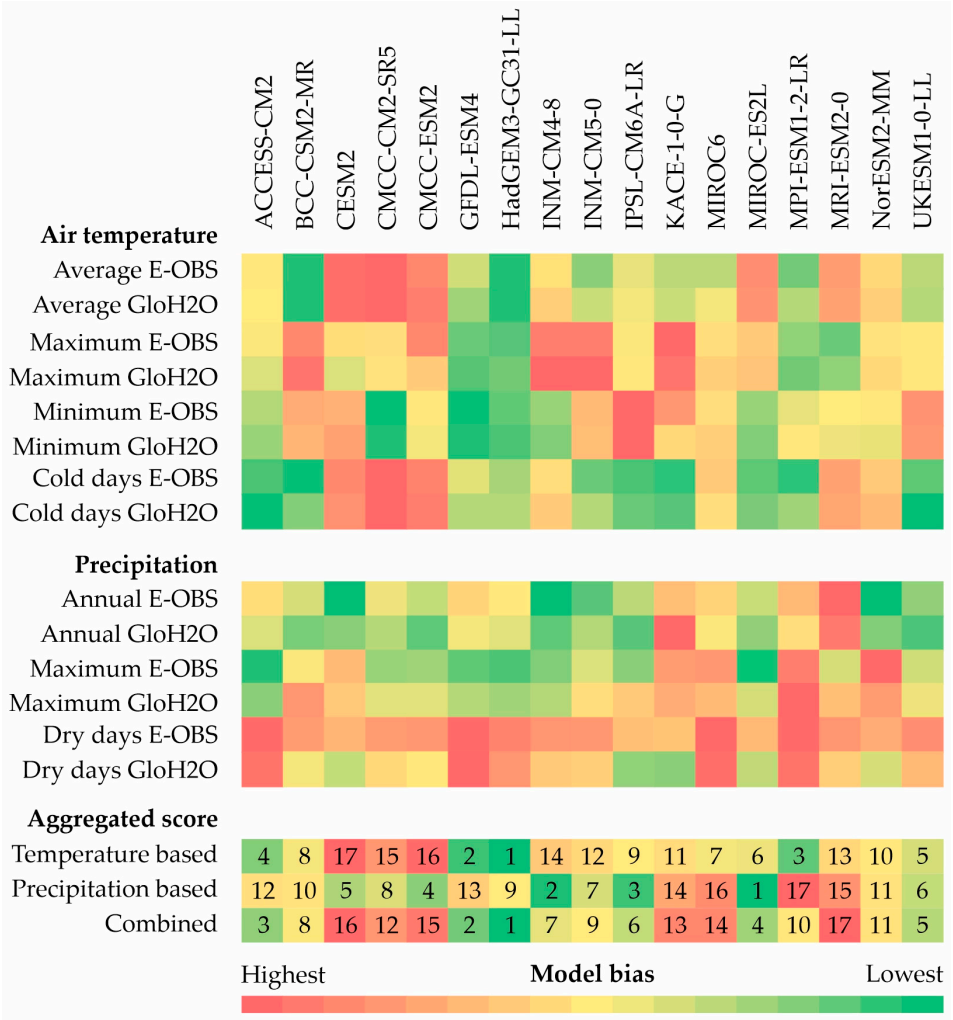

Figure 9. Model biases expressed by standardized deviations after gridded statistical downscaling compared to the raw simulation in the study area for 1981–2014, based on the downscaled air temperature and precipitation parameter data according to the historical datasets of E-OBS and GloH2O. The aggregated score represents the sum of the standardized deviations based on the analyzed parameters, the number indicates the consecutive rank of aggregated scores of the individual models according to the order from the lowest bias to the highest in terms of all models.

5. Discussion

In recent decades, high-resolution climate datasets such as GloH2O and E-OBS as well as reanalysis products such as ERA5 have become the basis for climate research and applied studies [10,35,36]. These datasets close gaps in observation networks and provide standardized, accessible climate data for different regions. GloH2O, for example, provides gridded observational data tailored to hydrological and climatic studies and applications, while E-OBS, derived from dense rain gauge networks, is widely used in Europe to study temperature and precipitation trends [37,38]. ERA5, developed by ECMWF, is particularly valuable for global studies as it provides physically consistent climate data and supports the modelling of hydroclimatic extremes and historical climate analyses [39]. The selection of data is crucial for high-resolution regional studies. Global climate models provide important baseline data, but their coarse resolution (e.g., ~1° × 1°) limits their ability to capture fine-scale climate variability [8]. Regional climate models provide higher spatial resolution (up to 10 km and in exceptional cases even higher), but their ability to adapt to updated climate scenarios is limited by computational costs. This gap emphasizes the need for alternative approaches such as statistical downscaling to refine the results of GCMs for

finer, more local grids. An important factor affecting the performance of the downscaled datasets is the representation of large-scale atmospheric factors in the GCMs. Features such as 500 mb geopotential height play a crucial role in driving local climate phenomena, including heat waves and droughts. Blocking systems, often characterized by persistent high-pressure anomalies, can lead to prolonged periods of extreme weather conditions, such as reduced precipitation and increased temperatures [40]. Differences in how GCMs simulate these large-scale patterns can contribute to variations in the downscaled data sets. Models that more accurately represent the dynamics and frequency of blocking systems are likely to produce downscaled data that are better suited to capture local climate extremes.

An effective downscaling method, Bias Correction and Constructed Analogues with Quantile Mapping reordering (BCCAQ), bridges the resolution gap by generating finer scaled grids based on GCM results [24,26,41]. This approach reduces modelling biases and improves spatial resolution, resulting in daily data that reflect regional climate dynamics more accurately than the raw GCM data. Gridded statistical downscaling requires a reliable historical data set to reflect local climatic features. Furthermore, the spatial resolution and data quality of these datasets, especially in topographically complex or data-limited areas, are crucial for the selection of a suitable dataset for regional climate studies. Our study, in which we compared E-OBS and GloH2O in statistical downscaling, shows the advantages of E-OBS in capturing local climatic features during the historical period and emphasizes the importance of regional datasets for accurate climate representation. Comparative analyses of data sets have repeatedly shown the importance of tailored data selection for effective downscaling and model validation. For example, studies on E-OBS and ERA5 in Europe show that E-OBS often performs better in areas with dense observation networks by capturing extreme events and spatial variability, while ERA5 performs better in data-poor regions where observation gaps reduce the reliability of E-OBS [30,42]. However, ERA5 tends to underestimate extreme events, indicating limitations in capturing local nuances compared to E-OBS, especially in densely monitored areas. High-resolution datasets such as E-OBS are therefore generally preferred for downscaling applications where accurate modelling of precipitation and temperature extremes is critical [43]. Conversely, the greater spatial coverage of GloH2O has the disadvantage of potentially smoothing local-scale variability, which is a drawback in regions with complicated microclimates. This pattern of regional strengths and weaknesses of different datasets is important for downscaling studies as it helps to identify which dataset is best suited to provide reliable baseline information for climate modelling. In downscaling applications, high-resolution datasets such as E-OBS are often favored as they can capture local variability, which is particularly valuable in studies of precipitation and temperature extremes [43].

Our results suggest that the performance of GloH2O in capturing extreme events, such as maximum precipitation, has several issues and should be further evaluated before application in impact studies. The effectiveness of statistical downscaling depends on the availability of high-quality observational data to serve as benchmarks for producing downscaling results [44]. Data settings such as E-OBS and GloH2O or others, with their regional focus and higher spatial resolution, provide crucial reference points for the downscaling process. E-OBS, for example, provides dense observational data for Europe, which helps to refine the accuracy of downscaling in different European climate zones [26,45]. Without such observational data, the reliability of downscaling results would be significantly lower. This emphasizes the fundamental role of databases that provide regional climate properties to improve model accuracy. However, using a reanalysis product such as GloH2O provides broader spatial coverage. This trade-off between observational precision and reanalysis coverage is an important consideration in our comparison of GloH2O and E-OBS. Other studies show that it is necessary to use multiple datasets to accurately model the effects of

climate. Iles et al. [8] compared CMIP5 and CORDEX simulations with E-OBS and found that the CMIP5 models generally underestimated precipitation extremes, while CORDEX tended to overestimate these values, especially at higher resolutions (12.5 km). The study also showed that the chosen observational dataset is sensitive, with the MESAN (MESoscale Analysis system) reanalysis [46] producing higher precipitation totals than E-OBS. These results illustrate how the choice of dataset significantly influences the model results and emphasize the need for careful selection of data sets when assessing regional climate trends. In hydrological modelling, the comparison of data sets is also of fundamental importance for the validation of runoff simulations.

GCMs consistently overestimate the frequency of light precipitation while underestimating the intensity of extreme precipitation, a phenomenon often referred to as the "drizzle effect". Several studies [47–49] suggest that GCMs have difficulty capturing extreme precipitation and that they often misrepresent heavy precipitation by simulating lower intensities at higher frequencies. Similarly, Zhang et al. [50] emphasize that GCMs systematically overestimate light precipitation. Comparisons between observations and models also show discrepancies in precipitation distribution. Observational data show that precipitation tends to be concentrated in intense events rather than the frequent light rainfall events modelled by GCMs [51]. The results of our study showed similar regularities, as the number of dry days (days without precipitation) was significantly increased by BCCAQ regardless of the applied database for corrections. This misrepresentation affects climate projections, especially hydrological assessments and predictions of extreme events. Studies suggest that accounting for changes in daily precipitation distribution [52] or reducing drizzle biases [50] improves model accuracy. Despite the progress, GCMs still face the challenge of accurately representing precipitation extremes. Eliminating these biases is crucial for refining climate projections, especially in water-scarce regions where precipitation patterns significantly influence climate impact assessments.

In particular, GCMs with high sensitivity, or those that predict a stronger transient climate response (TCR), may show a larger temperature increase in scenarios with increased greenhouse gas emissions than models with lower sensitivity. This is particularly important when it comes to extreme temperature events, as models with higher sensitivity tend to predict more extreme temperature anomalies in both the short and long term. In our study, the temperature extremes (minimum and maximum) simulated by the datasets were compared with the observed data and we found that datasets with higher climate sensitivity, such as some variants of the CMIP (Coupled Model Intercomparison Project) models, showed stronger warming trends. These models, which are often used in downscaling studies, generally show more pronounced temperature shifts under future emissions scenarios [53]. This is consistent with the observed patterns of temperature increase, but the magnitude of the temperature change can vary depending on model sensitivity. For example, the models with high sensitivity showed an increased frequency and intensity of heat waves in the simulated climate projections, indicating a stronger transient response of the climate to greenhouse gas forcing [54]. On the other hand, models with lower sensitivity, such as some of the reanalysis datasets, have captured milder temperature changes, which could underestimate the true extent of warming in certain regions. When selecting models for regional climate projections, it is important to take this difference in sensitivity into account, especially regarding temperature extremes. While E-OBS and GloH2O are valuable tools for understanding local climate dynamics, their ability to accurately represent future warming trends, especially in high emissions scenarios, needs to be understood in the context of their climate sensitivity. Incorporating climate sensitivity into the model assessment will ensure that temperature extremes, both minimum and

maximum, are not only modelled accurately in a historical context, but are also projected with an appropriate level of warming for future climate scenarios.

Ultimately, statistical downscaling, supported by high quality observational data, bridges the gap between global models and regional applications, improving both the accuracy and relevance of the models' results. By carefully selecting datasets that match regional climate characteristics, researchers can refine the results of GCMs, improve regional climate projections and provide effective adaptation strategies.

6. Conclusions

The study showed that 17 selected GCMs are able to represent the local climatic characteristics of the study area. Gridded statistical downscaling significantly improved the raw simulations of the GCMs and showed spatial differences in the applied improvements for the selected air temperature and precipitation parameters. There were several clear patterns that maximum temperatures were underestimated in the coastal zone and overestimated in the central and southern part of the study area by the raw GCM simulations. Accordingly, statistical downscaling increased the maximum temperature in the coastal zone for most models but reduced it in other areas. The opposite tendency was observed for the minimum temperatures, when the minimum temperatures were lowered in the coastal zone and significantly increased in the central and southern parts. Precipitation was also underestimated near the Baltic Sea, so that statistical downscaling increased its amount by up to 30% in certain models. The downscaling based on the E-OBS dataset provided more evenly distributed results with representation of local climatic features except for minimum temperature, as the contrast was higher in the southwestern part of the study area compared to GloH2O. Meanwhile, GloH2O provided higher amplitudes in the downscaled data compared to the raw simulations, especially for maximum precipitation, which exceeded 100% in several grid cells. In addition, large differences were observed between E-OBS and GloH2O for the dry days, as the E-OBS-based downscaling significantly increased the number of dry days.

Comparison of the databases and the air temperature and precipitation parameters used highlighted the most appropriate GCMs for the study region, based on the hypothesis that smaller differences between the raw and downscaled data indicate that the models are better able to represent the local climate in its uncorrected form. The aggregated score of the standardized deviations defined the GCMs with the best performance based on the air temperature and precipitation parameters. HadGEM3-GC31-LL, GFDL-ESM4 and ACCESS-CM2 were indicated as models that required the fewest corrections during statistical downscaling, but their representation of dry days was weaker than that of the other models. On the other hand, HadGEM3-GC31-LL together with MIROC-ES2L and UKESM1-0-LL were well balanced in terms of rank amplitude between air temperature and precipitation. The study showed that the ranking of aggregate scores is a valuable tool for evaluating relative performance between GCMs based on target parameters. When selecting, the target variables of interest should be prioritized as their complexity may hide the most important variables.

Author Contributions: Conceptualization, V.A. and K.G.; methodology, V.A. and K.G.; software, K.G.; formal analysis, V.A., K.G. and D.M.-L.; investigation, K.G. and D.J.; data curation, K.G. and D.J.; writing—original draft preparation, V.A., K.G., D.M.-L. and D.J.; writing—review and editing, V.A., K.G. and D.M.-L.; visualization, V.A. and K.G. All authors have read and agreed to the published version of the manuscript.

Funding: This research received no external funding.

Institutional Review Board Statement: Not applicable.

Informed Consent Statement: Not applicable.

Data Availability Statement: The data that support the findings of this study are available from the paper authors upon reasonable request.

Conflicts of Interest: The authors declare no conflicts of interest.

References

1. Parsons, L.A. Implications of CMIP6 Projected Drying Trends for 21st Century Amazonian Drought Risk. *Earth's Future* **2020**, *8*, e2020EF001608. [CrossRef]
2. Wu, Y.; Miao, C.; Fan, X.; Gou, J.; Zhang, Q.; Zheng, H. Quantifying the Uncertainty Sources of Future Climate Projections and Narrowing Uncertainties with Bias Correction Techniques. *Earth's Future* **2022**, *10*, e2022EF002963. [CrossRef]
3. Eum, H.-I.; Gupta, A.; Dibike, Y. Effects of Univariate and Multivariate Statistical Downscaling Methods on Climatic and Hydrologic Indicators for Alberta, Canada. *J. Hydrol.* **2020**, *588*, 125065. [CrossRef]
4. Illangasingha, S.; Koike, T.; Rasmy, M.; Tamakawa, K.; Matsuki, H.; Selvarajah, H. A Holistic Approach for Using Global Climate Model (GCM) Outputs in Decision Making. *J. Hydrol.* **2023**, *626*, 130213. [CrossRef]
5. Shukla, R.; Khare, D.; Kumar Dwivedi, A.; Rudra, R.P.; Palmate, S.S.; Ojha, C.S.P.; Singh, V.P. Evaluation of Statistical Downscaling Model's Performance in Projecting Future Climate Change Scenarios. *J. Water Clim. Chang.* **2023**, *14*, 3559–3595. [CrossRef]
6. Rampal, N.; Hobeichi, S.; Gibson, P.B.; Baño-Medina, J.; Abramowitz, G.; Beucler, T.; González-Abad, J.; Chapman, W.; Harder, P.; Gutiérrez, J.M. Enhancing Regional Climate Downscaling through Advances in Machine Learning. *Artif. Intell. Earth Syst.* **2024**, *3*, 230066. [CrossRef]
7. Chen, J.; Brissette, F.P.; Lucas-Picher, P.; Caya, D. Impacts of Weighting Climate Models for Hydro-Meteorological Climate Change Studies. *J. Hydrol.* **2017**, *549*, 534–546. [CrossRef]
8. Iles, C.E.; Vautard, R.; Strachan, J.; Joussaume, S.; Eggen, B.R.; Hewitt, C.D. The Benefits of Increasing Resolution in Global and Regional Climate Simulations for European Climate Extremes. *Geosci. Model Dev.* **2020**, *13*, 5583–5607. [CrossRef]
9. Boé, J.; Somot, S.; Corre, L.; Nabat, P. Large Discrepancies in Summer Climate Change over Europe as Projected by Global and Regional Climate Models: Causes and Consequences. *Clim. Dyn.* **2020**, *54*, 2981–3002. [CrossRef]
10. Williams, E.; Funk, C.; Peterson, P.; Tuholske, C. High Resolution Climate Change Observations and Projections for the Evaluation of Heat-Related Extremes. *Sci. Data* **2024**, *11*, 261. [CrossRef] [PubMed]
11. Eyring, V.; Bony, S.; Meehl, G.A.; Senior, C.A.; Stevens, B.; Stouffer, R.J.; Taylor, K.E. Overview of the Coupled Model Intercomparison Project Phase 6 (CMIP6) Experimental Design and Organization. *Geosci. Model Dev.* **2016**, *9*, 1937–1958. [CrossRef]
12. Riahi, K.; Van Vuuren, D.P.; Kriegler, E.; Edmonds, J.; O'Neill, B.C.; Fujimori, S.; Bauer, N.; Calvin, K.; Dellink, R.; Fricko, O.; et al. The Shared Socioeconomic Pathways and Their Energy, Land Use, and Greenhouse Gas Emissions Implications: An Overview. *Glob. Environ. Chang.* **2017**, *42*, 153–168. [CrossRef]
13. Intergovernmental Panel on Climate Change (IPCC). *Climate Change 2021—The Physical Science Basis: Working Group I Contribution to the Sixth Assessment Report of the Intergovernmental Panel on Climate Change*, 1st ed.; Cambridge University Press: Cambridge, UK, 2023; ISBN 9781009157896. [CrossRef]
14. Jacob, D.; Petersen, J.; Eggert, B.; Alias, A.; Christensen, O.B.; Bouwer, L.M.; Braun, A.; Colette, A.; Déqué, M.; Georgievski, G.; et al. EURO-CORDEX: New High-Resolution Climate Change Projections for European Impact Research. *Reg. Env. Chang.* **2014**, *14*, 563–578. [CrossRef]
15. Tapiador, F.J.; Navarro, A.; Moreno, R.; Sánchez, J.L.; García-Ortega, E. Regional Climate Models: 30 Years of Dynamical Downscaling. *Atmos. Res.* **2020**, *235*, 104785. [CrossRef]
16. Munawar, S.; Rahman, G.; Moazzam, M.F.U.; Miandad, M.; Ullah, K.; Al-Ansari, N.; Linh, N.T.T. Future Climate Projections Using SDSM and LARS-WG Downscaling Methods for CMIP5 GCMs over the Transboundary Jhelum River Basin of the Himalayas Region. *Atmosphere* **2022**, *13*, 898. [CrossRef]
17. Liu, Y.; Feng, J.; Yang, Z.; Hu, Y.; Li, J. Gridded Statistical Downscaling Based on Interpolation of Parameters and Predictor Locations for Summer Daily Precipitation in North China. *J. Appl. Meteorol. Climatol.* **2019**, *58*, 2295–2311. [CrossRef]
18. Sunyer, M.A.; Gregersen, I.B.; Rosbjerg, D.; Madsen, H.; Luchner, J.; Arnbjerg-Nielsen, K. Comparison of Different Statistical Downscaling Methods to Estimate Changes in Hourly Extreme Precipitation Using RCM Projections from ENSEMBLES: STATISTICAL DOWNSCALING METHODS FOR EXTREME PRECIPITATION. *Int. J. Clim.* **2015**, *35*, 2528–2539. [CrossRef]
19. Zhang, Q.; Shi, P.; Singh, V.P.; Fan, K.; Huang, J. Spatial Downscaling of TRMM -based Precipitation Data Using Vegetative Response in Xinjiang, China. *Int. J. Climatol.* **2017**, *37*, 3895–3909. [CrossRef]
20. Zhu, X.; Qiu, X.; Zeng, Y.; Ren, W.; Tao, B.; Pan, H.; Gao, T.; Gao, J. High-resolution Precipitation Downscaling in Mountainous Areas over China: Development and Application of a Statistical Mapping Approach. *Int. J. Climatol.* **2018**, *38*, 77–93. [CrossRef]
21. Werner, A.T.; Cannon, A.J. Hydrologic Extremes—An Intercomparison of Multiple Gridded Statistical Downscaling Methods. *Hydrol. Earth Syst. Sci.* **2016**, *20*, 1483–1508. [CrossRef]

22. Cannon, A.J.; Sobie, S.R.; Murdock, T.Q. Bias Correction of GCM Precipitation by Quantile Mapping: How Well Do Methods Preserve Changes in Quantiles and Extremes? *J. Clim.* **2015**, *28*, 6938–6959. [CrossRef]
23. Sobie, S.R.; Murdock, T.Q. High-Resolution Statistical Downscaling in Southwestern British Columbia. *J. Appl. Meteorol. Climatol.* **2017**, *56*, 1625–1641. [CrossRef]
24. Fauzi, F.; Kuswanto, H.; Atok, R.M. Bias Correction and Statistical Downscaling of Earth System Models Using Quantile Delta Mapping (QDM) and Bias Correction Constructed Analogues with Quantile Mapping Reordering (BCCAQ). *J. Phys. Conf. Ser.* **2020**, *1538*, 012050. [CrossRef]
25. Murdock, T.Q.; Cannon, A.J.; Sobie, S.R. *Statistical Down-Scaling of Future Climate Projections for North America*; Report on Contract No: KM040-131148/A; Prepared for Environment Canada; Pacific Climate Impacts Consortium: Victoria, BC, Canada, 2014.
26. Gebrechorkos, S.; Leyland, J.; Slater, L.; Wortmann, M.; Ashworth, P.J.; Bennett, G.L.; Boothroyd, R.; Cloke, H.; Delorme, P.; Griffith, H.; et al. A High-Resolution Daily Global Dataset of Statistically Downscaled CMIP6 Models for Climate Impact Analyses. *Sci. Data* **2023**, *10*, 611. [CrossRef]
27. Jalili Pirani, F.; Bakhtiari, S.; Najafi, M.R.; Shrestha, R.R.; Nouri, M.S. The Effects of Climate Change on Flood-Generating Mechanisms in the Assiniboine and Red River Basins. In Proceedings of the AGY Fall Meeting 2021, New Orleans, LA, USA, 13–17 December 2021. NH15F-0514.
28. Geography, S.O.; Gebrechorkos, S.; Leyland, J.; Darby, S.; Parsons, D. *High-Resolution Daily Global Climate Dataset of BCCAQ Statistically Downscaled CMIP6 Models for the EVOFLOOD Project*; NERC EDS Centre for Environmental Data Analysis, University of Southampton: Southampton, UK, 2022.
29. Copernicus Climate Change Service E-OBS Daily Gridded Meteorological Data for Europe from 1950 to Present Derived from in-Situ Observations 2020. Available online: https://cds.climate.copernicus.eu/datasets/insitu-gridded-observations-europe?tab=overview (accessed on 26 August 2024). [CrossRef]
30. Bandhauer, M.; Isotta, F.; Lakatos, M.; Lussana, C.; Båserud, L.; Izsák, B.; Szentes, O.; Tveito, O.E.; Frei, C. Evaluation of Daily Precipitation Analyses in E-OBS (V19.0e) and ERA5 by Comparison to Regional High-resolution Datasets in European Regions. *Int. J. Climatol.* **2022**, *42*, 727–747. [CrossRef]
31. Vrac, M.; Vaittinada Ayar, P. Influence of Bias Correcting Predictors on Statistical Downscaling Models. *J. Appl. Meteorol. Climatol.* **2017**, *56*, 5–26. [CrossRef]
32. Baño-Medina, J.; Manzanas, R.; Gutiérrez, J.M. On the Suitability of Deep Convolutional Neural Networks for Continental-Wide Downscaling of Climate Change Projections. *Clim. Dyn.* **2021**, *57*, 2941–2951. [CrossRef]
33. Maurer, E.P.; Hidalgo, H.G.; Das, T.; Dettinger, M.D.; Cayan, D.R. The Utility of Daily Large-Scale Climate Data in the Assessment of Climate Change Impacts on Daily Streamflow in California. *Hydrol. Earth Syst. Sci.* **2010**, *14*, 1125–1138. [CrossRef]
34. Hunter, R.D.; Meentemeyer, R.K. Climatologically Aided Mapping of Daily Precipitation and Temperature. *J. Appl. Meteorol.* **2005**, *44*, 1501–1510. [CrossRef]
35. Behnke, R.; Vavrus, S.; Allstadt, A.; Albright, T.; Thogmartin, W.E.; Radeloff, V.C. Evaluation of Downscaled, Gridded Climate Data for the Conterminous United States. *Ecol. Appl.* **2016**, *26*, 1338–1351. [CrossRef] [PubMed]
36. Mankin, K.R.; Mehan, S.; Green, T.R.; Barnard, D.M. Review of Gridded Climate Products and Their Use in Hydrological Analyses Reveals Overlaps, Gaps, and Need for More Objective Approach to Model Forcings. *Hydrol. Earth Syst. Sci. Discuss.* **2025**, *29*, 85–108. [CrossRef]
37. Cornes, R.C.; Van Der Schrier, G.; Van Den Besselaar, E.J.M.; Jones, P.D. An Ensemble Version of the E-OBS Temperature and Precipitation Data Sets. *JGR Atmos.* **2018**, *123*, 9391–9409. [CrossRef]
38. Moreno, A.; Hasenauer, H. Spatial Downscaling of European Climate Data. *Int. J. Climatol.* **2016**, *36*, 1444–1458. [CrossRef]
39. Brunner, M.I.; Götte, J.; Schlemper, C.; Van Loon, A.F. Hydrological Drought Generation Processes and Severity Are Changing in the Alps. *Geophys. Res. Lett.* **2023**, *50*, e2022GL101776. [CrossRef]
40. Bakke, S.J.; Ionita, M.; Tallaksen, L.M. Recent European Drying and Its Link to Prevailing Large-Scale Atmospheric Patterns. *Sci. Rep.* **2023**, *13*, 21921. [CrossRef] [PubMed]
41. Rettie, F.M.; Gayler, S.; Weber, T.K.D.; Tesfaye, K.; Streck, T. High-Resolution CMIP6 Climate Projections for Ethiopia Using the Gridded Statistical Downscaling Method. *Sci. Data* **2023**, *10*, 442. [CrossRef]
42. Hagemann, S.; Stacke, T. Complementing ERA5 and E-OBS with High-Resolution River Discharge over Europe. *Oceanologia* **2023**, *65*, 230–248. [CrossRef]
43. Laiti, L.; Mallucci, S.; Piccolroaz, S.; Bellin, A.; Zardi, D.; Fiori, A.; Nikulin, G.; Majone, B. Testing the Hydrological Coherence of High-Resolution Gridded Precipitation and Temperature Data Sets. *Water Resour. Res.* **2018**, *54*, 1999–2016. [CrossRef]
44. Sun, Y.; Deng, K.; Ren, K.; Liu, J.; Deng, C.; Jin, Y. Deep Learning in Statistical Downscaling for Deriving High Spatial Resolution Gridded Meteorological Data: A Systematic Review. *ISPRS J. Photogramm. Remote Sens.* **2024**, *208*, 14–38. [CrossRef]
45. Caldas-Alvarez, A.; Feldmann, H.; Lucio-Eceiza, E.; Pinto, J.G. Convection-Parameterized and Convection-Permitting Modelling of Heavy Precipitation in Decadal Simulations of the Greater Alpine Region with COSMO-CLM. *Weather Clim. Dynam.* **2023**, *4*, 543–565. [CrossRef]

46. Landelius, T.; Dahlgren, P.; Gollvik, S.; Jansson, A.; Olsson, E. A High-resolution Regional Reanalysis for Europe. Part 2: 2D Analysis of Surface Temperature, Precipitation and Wind. *Q. J. R. Meteorol. Soc.* **2016**, *142*, 2132–2142. [CrossRef]
47. Niu, X.; Wang, S.; Tang, J.; Lee, D.; Gutowski, W.; Dairaku, K.; McGregor, J.; Katzfey, J.; Gao, X.; Wu, J.; et al. Ensemble Evaluation and Projection of Climate Extremes in China Using RMIP Models. *Int. J. Climatol.* **2018**, *38*, 2039–2055. [CrossRef]
48. He, S.; Yang, J.; Bao, Q.; Wang, L.; Wang, B. Fidelity of the Observational/Reanalysis Datasets and Global Climate Models in Representation of Extreme Precipitation in East China. *J. Clim.* **2019**, *32*, 195–212. [CrossRef]
49. Wang, L.; Zhang, J.; Shu, Z.; Wang, Y.; Bao, Z.; Liu, C.; Zhou, X.; Wang, G. Evaluation of the Ability of CMIP6 Global Climate Models to Simulate Precipitation in the Yellow River Basin, China. *Front. Earth Sci.* **2021**, *9*, 751974. [CrossRef]
50. Zhang, Z.; Wang, Y.; Zhang, G.J.; Xing, C.; Xia, W.; Yang, M. Light Rain Exacerbates Extreme Humid Heat. *Nat. Commun.* **2024**, *15*, 7326. [CrossRef] [PubMed]
51. Pendergrass, A.G.; Knutti, R. The Uneven Nature of Daily Precipitation and Its Change. *Geophys. Res. Lett.* **2018**, *45*, 11980–11988. [CrossRef]
52. Mpelasoka, F.S.; Chiew, F.H.S. Influence of Rainfall Scenario Construction Methods on Runoff Projections. *J. Hydrometeorol.* **2009**, *10*, 1168–1183. [CrossRef]
53. Tefera, G.W.; Ray, R.L.; Wootten, A.M. Evaluation of Statistical Downscaling Techniques and Projection of Climate Extremes in Central Texas, USA. *Weather Clim. Extrem.* **2024**, *43*, 100637. [CrossRef]
54. Petrovic, D.; Fersch, B.; Kunstmann, H. Heat Wave Characteristics: Evaluation of Regional Climate Model Performances for Germany. *Nat. Hazards Earth Syst. Sci.* **2024**, *24*, 265–289. [CrossRef]

Disclaimer/Publisher's Note: The statements, opinions and data contained in all publications are solely those of the individual author(s) and contributor(s) and not of MDPI and/or the editor(s). MDPI and/or the editor(s) disclaim responsibility for any injury to people or property resulting from any ideas, methods, instructions or products referred to in the content.